

MICROCOPY RESOLUTION TEST CHART  
NATIONAL BUREAU OF STANDARDS-1963-A

12

AD-A172 347

OFFICE OF NAVAL RESEARCH

Contract N00014-79-C-0647

TECHNICAL REPORT #24

"ON THE PYRAZINE AND PYRAZINE-PYRIMIDINE DIMERS"

by

J. Wanna and E.R. Bernstein

Prepared for Publication

in the

Journal of Chemical Physics

Department of Chemistry  
Colorado State University  
Fort Collins, Colorado 80523

DTIC  
ELECTE  
SEP 22 1986  
S B D

1 JUNE  
May 1986

Reproduction in whole or in part is permitted for any purpose of the United States Government.

This document has been approved for public release and sale; its distribution is unlimited.

DTIC FILE COPY

*AD-A17334*

REPORT DOCUMENTATION PAGE

1a. REPORT SECURITY CLASSIFICATION			1b. RESTRICTIVE MARKINGS			
2a. SECURITY CLASSIFICATION AUTHORITY			3. DISTRIBUTION / AVAILABILITY OF REPORT Approved for public release; distribution unlimited.			
2b. DECLASSIFICATION / DOWNGRADING SCHEDULE Unclassified			5. MONITORING ORGANIZATION REPORT NUMBER(S)			
4. PERFORMING ORGANIZATION REPORT NUMBER(S) N00014-79-C-0647			7a. NAME OF MONITORING ORGANIZATION			
6a. NAME OF PERFORMING ORGANIZATION Colorado State University		6b. OFFICE SYMBOL (if applicable)		7b. ADDRESS (City, State, and ZIP Code)		
6c. ADDRESS (City, State, and ZIP Code) Department of Chemistry Fort Collins, Colorado 80523			9. PROCUREMENT INSTRUMENT IDENTIFICATION NUMBER N00014-79-C-0647			
8a. NAME OF FUNDING / SPONSORING ORGANIZATION U.S. Army Research Office		8b. OFFICE SYMBOL (if applicable)		10. SOURCE OF FUNDING NUMBERS		
8c. ADDRESS (City, State, and ZIP Code) Post Office Box 12211 Research Triangle Park, NC 27709			PROGRAM ELEMENT NO.	PROJECT NO.	TASK NO.	WORK UNIT ACCESSION NO.
11. TITLE (Include Security Classification) "On the Pyrazine and Pyrazine-Pyrimidine Dimers"						
12. PERSONAL AUTHOR(S) J. Wanna and E.R. Bernstein						
13a. TYPE OF REPORT Technical Report		13b. TIME COVERED FROM TO		14. DATE OF REPORT (Year, Month, Day) June 1, 1986		15. PAGE COUNT 31
16. SUPPLEMENTARY NOTATION The view, opinions, and/or findings contained in this report are those of the author(s) and should not be construed as an official Department of the Army position, policy, or decision, unless so designated by other documentation.						
17. COSATI CODES			18. SUBJECT TERMS (Continue on reverse if necessary and identify by block number)			
FIELD	GROUP	SUB-GROUP	<i>sub 4 sub 4</i>			
19. ABSTRACT (Continue on reverse if necessary and identify by block number) Spectra of the pyrazine-d <sub>4</sub> , pyrazine-h <sub>4</sub> -pyrazine-d <sub>4</sub> and pyrazine-d <sub>4</sub> -pyrimidine dimer are obtained and analyzed with the help of Lennard-Jones-hydrogen-bonding (LJ-HB) potential energy calculations. The pyrazine isotopic hetero- and homo-dimers possess nearly identical spectra with the exception that the perpendicular dimer features are displaced to the red by 11 cm <sup>-1</sup> . Exchange or exciton interactions in this system are vanishingly small (less than 1/cm <sup>-1</sup> ). The geometries suggested by the isotopically substituted pyrazine dimer spectra are the same as those found for the pyrazine-h <sub>4</sub> homo-dimer: a parallel planar hydrogen bonded and a perpendicular dimer. The pyrazine-d <sub>4</sub> - and pyrazine-h <sub>4</sub> -pyrimidine dimer spectra are quite complicated. These spectra can be assigned as rising from one parallel stacked head-to-tail displaced dimer, one parallel planar dimer, and 3 perpendicular dimers based on comparisons with spectra of the pyrazine and pyrimidine dimers.						
20. DISTRIBUTION / AVAILABILITY OF ABSTRACT <input checked="" type="checkbox"/> UNCLASSIFIED/UNLIMITED <input type="checkbox"/> SAME AS RPT <input type="checkbox"/> DTIC USERS				21. ABSTRACT SECURITY CLASSIFICATION UNCLASSIFIED		
22a. NAME OF RESPONSIBLE INDIVIDUAL Elliot R. Bernstein				22b. TELEPHONE (Include Area Code) 303-491-6347		22c. OFFICE SYMBOL

86 0 18 001

## I. Introduction.

The study of dimers of simple organic systems has a number of motivations. Dimers are of interest in their own right for the investigation of geometry, energy levels, intermolecular interactions and vibrational dynamics. In addition, dimers can serve as models for various condensed phase systems and nonrigid, flexible molecules. Dimer formation must be an essential process in the early stages of the nucleation and growth of condensed phases. Condensed phase dynamics and molecular rearrangements can be elucidated through dimer intramolecular vibrational redistribution and vibrational predissociation studies. Various types of dimers have been studied by supersonic molecular jet laser optical spectroscopy.<sup>1,2,3</sup>

Among the various supersonic molecular jet optical techniques available for the study of clusters in general, we have invariably employed two color time of flight mass spectroscopy (2-color TOFMS) for the investigation of dimers. The 2-color TOFMS technique allows the optical spectrum of a species belonging to a particular mass to be recorded. This is essential for the spectroscopic characterization of isotopic species and for dimers with different geometries but identical masses. The 2-color TOFMS technique yields both mass and wavelength resolution in a single experiment. The spectra of (benzene)<sub>2</sub><sup>2</sup>, (toluene)<sub>2</sub><sup>1a</sup>, (toluene-benzene)<sub>2</sub><sup>1a</sup>, (pyrazine)<sub>2</sub><sup>3</sup>, (pyrimidine)<sub>2</sub><sup>3</sup> and many of their deuterated analogues have been recorded and analyzed with this technique. Along with the experimental data, potential energy calculations employing Lennard-Jones (LJ, 1-6-12) potential functions are used to generate minimum energy configurations for the dimers. A hydrogen bonding term of the form (10-12) replaces the LJ (6-12) form if a hydrogen bonding interaction is possible for a pair of atoms. Details of this procedure, atom-atom potential parameters, and the calculational techniques are discussed in previous publications from our laboratory.<sup>3,4</sup>



✓  
PER  
CALL  
JC

In the case of protonated pyrazine, both the experimental results and the potential energy calculations generate a consistent set of conclusions for the dimer geometries. The calculations produce three distinct geometries for the pyrazine dimer: a hydrogen bonded planar configuration with a nitrogen of each pyrazine coordinated to a hydrogen of its partner; a perpendicular configuration with two hydrogens of the stem pyrazine oriented toward the nitrogens of the base pyrazine; and parallel stacked pyrazine with the two pyrazines rotated  $\pi/4$  with respect to one another. Observed spectral features can be assigned to the first two configurations, but not the third. The latter configuration can form an excimer and may well have no sharp observable features within thousands of wavenumbers of the pyrazine  $0_0^0$ .

The experimental observations for the pyrimidine dimers are much more complex than those of pyrazine, but, nonetheless, the calculations still render an accurate, logical, and self consistent assignment of these data. Calculations find a head-to-tail parallel stacked and displaced configuration, another parallel stacked configuration but with the two pyrimidine molecules rotated  $\pi/4$  with respect to one another, and four distinct, hydrogen bonded planar configurations. Unlike the case of pyrazine, no perpendicular configurations can be calculated with the potential employed. The four planar configurations are expected to be blue shifted from the pyrimidine origin and can be readily identified in the spectrum. The parallel stacked displaced, head-to-tail configuration can be assigned to a single feature with a large red shift ( $\Delta \sim -170 \text{ cm}^{-1}$ ). The stacked and rotated configuration is not assigned to a spectroscopic feature and is presumed to form an excimer.

Since both spectroscopic data and calculational results present a consistent picture of the pyrazine and pyrimidine dimers, the LJ potential form proves of great value in making assignments and in understanding the nature of the dimers in general.

The set of experiments reported herein are designed to examine further the pyrazine and pyrimidine dimers. Of particular interest with regard to the above results for the individual dimers, is the existence of perpendicular dimer structures for pyrimidine with other molecules. The dimers of pyrazine and pyrimidine, as well as their mixed dimers, all have the same mass and thus the most useful experiment for the mixed dimer employs pyrazine-d<sub>4</sub> rather than pyrazine-h<sub>4</sub>. The selective use of isotopically enriched molecules displays another significant advantage of 2-color TOFMS techniques. Pyrazine-d<sub>4</sub> is chosen rather than pyrimidine-d<sub>4</sub> because of its ready commercial availability.

As a consequence, pyrazine-d<sub>4</sub> and pyrazine-d<sub>4</sub>-h<sub>4</sub> dimers are also studied and reported. These latter dimers have spectra similar to the pyrazine-h<sub>4</sub> dimer, as would be expected based on the LJ potential calculations.

The mixed pyrazine-d<sub>4</sub>-pyrimidine-h<sub>4</sub> dimers, on the other hand, do evidence spectra which are quite different from those of the homo dimers. In order to interpret and assign fully the mixed pyrazine-d<sub>4</sub>-pyrimidine-h<sub>4</sub> dimer spectra, use is also made of the pyrazine-h<sub>4</sub>-pyrimidine-h<sub>4</sub> dimer spectrum. While these latter spectra are even more congested than the pyrazine-d<sub>4</sub>-pyrimidine-h<sub>4</sub> spectra, the combination of the spectra of all four dimers is sufficient, in conjunction with the calculation, to assign self consistently all features with reasonable certainty. The pyrazine-pyrimidine dimer system includes one planar, one stacked and three perpendicular configurations.

## II. Experimental Procedures.

The experimental apparatus and procedures for the supersonic molecular jet 2-color TOFMS study of dimers have been described in earlier publications<sup>4,5</sup> in considerable detail. Briefly, the dimers are generated with a pulsed valve having an 0.5 mm orifice. After the beam is skimmed, it is intersected by two

pulsed laser beams 7.5 cm downstream from the valve. The two laser beams and the molecular beam intersect between the accelerator plates of the TOFMS; one laser excites the dimer to its first excited singlet state ( $S_1$ ) and the second laser generates the dimer ion from  $S_1$ . The signal from the mass detector is monitored on a transient digitizer or a boxcar averager. The output of these devices then goes to a computer for further averaging and storage. The computer scans the lasers and controls the time evolution of the experiment.

The lasers are two Nd/YAG pumped dye lasers, the outputs of which are doubled and/or mixed with the 1.064  $\mu\text{m}$  pump beam to achieve the proper independent final frequencies for the  $S_1 + S_0$  and ion +  $S_1$  transitions. The pump dye laser employs DCM dye and the ionization dye laser employs R590 dye; both outputs are doubled.

The samples are treated as discussed in previous publications. The backing pressure for the nozzle is typically 120 psig.

The calculational procedure and potential energy terms have been given in an earlier publication;<sup>4</sup> the constants employed in the potential can be found in refs. 4, 5, 6. No parameter fitting is done in these calculations and thus they represent an independent set of data to aid in the spectral analysis.

### III. Results.

#### A. Pyrazine- $d_4$ Dimer.

The pyrazine- $d_4$  dimer spectra taken at two different ionization energies are shown in fig. 1. Four features disappear in the spectrum of the dimer as the ionization energy is lowered from ca. 43,600 to 42,300  $\text{cm}^{-1}$ ; these are located at shifts of -11.5, +11.5, 25.5 and 64.1  $\text{cm}^{-1}$  from the pyrazine- $d_4$  monomer  $O_0^0$  transition at 31030.4  $\text{cm}^{-1}$ . The relatively intense features that remain at the lower ionization energy are located at shifts of -26.9, -6.4, +31.0 and +45.9  $\text{cm}^{-1}$  with respect to the pyrazine- $d_4$

$0_0^0$  transition. From this dependence of the spectrum upon ionization energy, one concludes that at least two configurations of the dimer are present in the molecular jet expansion. A similar dependence on ionization energy has been reported for pyrazine- $h_4$  dimer.<sup>3</sup> Table I summarizes these data.

Dimer spectra corresponding to the other pyrazine- $d_4$  vibronic origins  $10_0^1$  and  $6a_0^1$  are shown in fig. 2 along with the  $0_0^0$  spectrum. Note that a few of the features in these vibronic spectra do not appear to vary in shift or relative intensity as a function of the pyrazine vibronic transition observed. Comparing all three of these vibronic transitions to one another and those obtained for the pyrazine- $h_4$  dimer,<sup>3</sup> one concludes that the features at  $-26.9$ ,  $-11.5$  and  $+31.0$   $\text{cm}^{-1}$  are all pyrazine- $d_4$  dimer origins ( $0$ ,  $15.4$ , and  $57.9$   $\text{cm}^{-1}$  relative to the scale in fig. 2) for each vibronic transition. Table I presents the energies of and assignments for these features.

Potential energy calculations utilizing a LJ function with hydrogen bonding terms give three configurations for the pyrazine dimer. Two of these configurations are depicted in fig. 3 with their calculated binding energies. One configuration is planar and the other is perpendicular. The third configuration, not shown in fig. 3, is parallel stacked with the two pyrazines rotated  $90^\circ$  with respect to each other. This third configuration does not apparently contribute to the observed dimer spectrum probably due to excimer formation.

#### B. Pyrazine- $h_4$ -Pyrazine- $d_4$ Dimer.

The energy difference between the monomer origins of pyrazine- $h_4$  ( $30876.0$   $\text{cm}^{-1}$ ) and pyrazine- $d_4$  ( $31030.4$   $\text{cm}^{-1}$ ) is  $154.4$   $\text{cm}^{-1}$ . Such a large separation between monomer origins allows the excitation of either the protonated or deuterated pyrazine moieties to be individually accessed and identified: spectra of one excitation do not interfere with or congest the spectra of the other excitation. The top part of fig. 4 shows the spectrum.

associated with excitation of the deuterated pyrazine of the isotopic mixed dimer, while the lower part of the figure displays spectra associated with excitation of the protonated pyrazine of the mixed dimer. The spectra of the two different isotopes in the dimer are nearly identical. Table II lists the energies and assignments for these features. The origins for the different dimer configurations are found shifted from their respective monomer transitions by  $-38$ ,  $-12$  and  $+23$   $\text{cm}^{-1}$ . These features are also nearly identical to the two homo-dimers, with the exception of an  $11$   $\text{cm}^{-1}$  red shift for the low and high energy pair of features.

Calculated geometries of the isotopic hetero-dimers are of course identical to those of the homo-dimers. The potential energy employed to obtain geometries and binding energies does not depend on isotopic substitution.

#### C. Pyrazine- $\text{d}_4$ -Pyrimidine Dimer.

The  $0_0^0$  transition of the pyrimidine monomer at  $31072.7$   $\text{cm}^{-1}$  is only about  $42$   $\text{cm}^{-1}$  to the blue of the pyrazine- $\text{d}_4$  monomer  $0_0^0$  transition at  $31030.4$   $\text{cm}^{-1}$ . This spectrum is shown in two segments in fig. 5. The first section depicts the spectrum close to the monomer origins and the second section depicts the spectrum  $-300$   $\text{cm}^{-1}$  to blue of the pyrazine- $\text{d}_4$  monomer origin. If one compares the spectrum near the origin of the pyrazine- $\text{d}_4$ -pyrimidine hetero-dimer (first section of fig. 5) to that of the pyrazine- $\text{h}_4$ -pyrazine- $\text{d}_4$  hetero-dimer (fig. 4), one concludes that some of the features are apparently the same in both spectra. The supposed common features occur at shifts of  $-39.6$ ,  $23.2$  and  $31.4$   $\text{cm}^{-1}$  in the pyrazine- $\text{d}_4$ -pyrimidine spectrum (see fig. 5 and Table III). Another set of features are found at shifts of  $-104.3$ ,  $-79.8$ ,  $-62.7$  and  $-51.2$   $\text{cm}^{-1}$  with respect to the pyrazine- $\text{d}_4$   $0_0^0$  transition; these latter features are not observed in the pyrazine- $\text{h}_4$ -pyrazine- $\text{d}_4$  hetero-dimer spectrum. A final set of features for

the pyrazine-d<sub>4</sub>-pyrimidine hetero-dimer is displayed in the second segment of fig. 5, 300 cm<sup>-1</sup> to the blue of the monomer origins. The two intense features in this latter region are shifted 219.5 and 261.7 cm<sup>-1</sup> from the pyrimidine O<sub>0</sub><sup>0</sup> transition. For simplicity, we present in fig. 6 a stick diagram representing the spectra of the four possible homo- and hetero-dimers. Given these comparisons, one concludes that the features at -39.6, 23.3 and 31.4 cm<sup>-1</sup> with respect to the pyrazine-d<sub>4</sub> origin are associated with (two) dimer origins of a nature similar to those assigned for the pyrazine dimer. The intense features to the red and blue of this group have no counterparts in the homo- or hetero-dimers of pyrazine itself, and must therefore be associated with the pyrimidine moiety.

To assign the remainder of the pyrazine-d<sub>4</sub>-pyrimidine hetero-dimer spectrum, more information is quite helpful. The pyrazine-h<sub>4</sub>-pyrimidine-h<sub>4</sub> hetero-dimer spectra are studied by 2-color TOFMS to provide this additional input; however, in this instance, all three h<sub>4</sub>-dimers of pyrazine and pyrimidine are observed without mass discrimination. Since the homo-dimers have been studied and their spectra reported, one may uniquely identify the pyrazine-h<sub>4</sub>-pyrimidine-h<sub>4</sub> spectrum and compare it to that of the pyrazine-d<sub>4</sub>-pyrimidine spectra. Hence, those features common to both pyrazine-h<sub>4</sub> and pyrazine-d<sub>4</sub>-pyrimidine hetero-dimer spectra with roughly constant shifts from the pyrimidine O<sub>0</sub><sup>0</sup> transition can be confidently assigned to the pyrimidine moiety. These specific assignments will be made in the discussion section to follow.

A LJ potential energy calculation with a hydrogen bonding term produces six possible configurations for the mixed dimer. Two of these configurations are displayed in fig. 7 with their calculated binding energies. The largest binding energy configuration for the hetero-dimer is parallel stacked with the pyrimidine center of mass displaced 0.61 Å<sup>0</sup> from the pyrazine

center of mass and the two ring planes separated by  $3.3 \text{ \AA}$ . The two meta-position carbons of the pyrimidine ring are situated nearly above the nitrogens of the pyrazine ring. The other configuration depicted in fig. 7 is a planar hydrogen bonded geometry with the most "acidic" or electropositive hydrogen on pyrimidine and one hydrogen on pyrazine forming two  $\text{N}\cdots\text{H}$  hydrogen bonds. The center-to-center molecular distance in this configuration is  $5.7 \text{ \AA}$  and the  $\text{H}\cdots\text{N}$  distance is  $\sim 2.3 \text{ \AA}$ . An additional parallel stacked undisplaced configuration is not shown: it has the para-position carbons of pyrimidine above the nitrogens of pyrazine. This configuration is not assigned in the spectrum.

In addition to these configurations the LJ calculations produce three distinct perpendicular geometries for the pyrazine-pyrimidine dimer. These are shown in fig. 8. Configuration I has pyrimidine at the base and pyrazine at the stem of the structure with a center-to-center distance of  $4.5 \text{ \AA}$ . The second and third configurations (fig. 8, II and III) both have pyrazine at the base and pyrimidine at the stem. The center-to-center distance for these geometries is  $4.9 \text{ \AA}$  and the  $\text{N}\cdots\text{H}$  hydrogen bonding distance varies from  $2.8$  to  $3.0 \text{ \AA}$  in both dimers. Configurations II and III of fig. 8 are nearly identical except for a rotation of pyrimidine about an axis perpendicular to the pyrazine plane.

These calculations can thus produce pyrazine or pyrimidine molecules in either the stem or base position of a perpendicular hetero-pyrazine-pyrimidine dimer.

#### IV. Discussion.

In this section we attempt the sometimes difficult task of assigning observed spectroscopic features of the various dimers to the calculated configurations. In all instances such a unique correspondence is possible. The specific assignments are summarized in Tables I, II, III and the con-

figurations to which the assignments refer are found in figs. 3, 7, 8. For added assistance, the pyrazine-d<sub>4</sub>-pyrimidine dimer spectrum (fig. 5) has assignments written on it directly.

A. Pyrazine-d<sub>4</sub> Dimer.

Spectra of the pyrazine-d<sub>4</sub> and pyrazine-h<sub>4</sub><sup>3</sup> dimer are quite similar in terms of ionization energy dependence and spectroscopic feature position and intensity. The features that vanish at low ionization energy (fig. 1) are assigned to a single dimer origin with its associated vdW vibronic modes. The spectra are summarized for easy comparison in fig. 6. The dimer configuration with the higher ionization energy is most likely a symmetrical one because only one clear origin is associated with it. We have previously argued<sup>1a,2,3</sup> that different dimer geometries should possess different ionization energies depending on the involvement of the  $\pi$ -electron cloud in the ion "solvation" process.

Therefore, based on the above reasoning and comparisons, the features associated with the high ionization energy cluster ( $-11.5 \text{ cm}^{-1}$  cluster  $0_0^0$ ) are attributed to the dimer with the planar configuration (I in fig. 3). The planar dimer can be argued to have the higher ionization because the  $\pi$ -system is not involved in the bonding. Note that the planar hydrogen bonded configuration is composed of two symmetry equivalent molecules and thus only one spectroscopic origin is expected for this dimer.

The other two features previously identified as origins ( $-26.9$  and  $+31.0 \text{ cm}^{-1}$ ) are assigned to the perpendicular configuration (II in fig. 3). The red shifted feature is suggested to be due to the base pyrazine and the blue shifted feature is associated with the stem pyrazine. These latter detailed assignments are made under the assumption that red shifts are caused by  $\pi$ -cloud interactions and blue shifts are caused by hydrogen bonding interactions. Table I lists these and other assignments for the pyrazine-d<sub>4</sub>

homo-dimer. The causes of cluster shifts are discussed in previous publications from this laboratory.<sup>1a, 2-5</sup>

From fig. 2 and Table I one can also see that strong vibronic coupling exists between the pyrazine  $6a^1$  and  $10a^1$  modes and the vdW modes even though the cluster vibronic origins at the pyrazine vibronic levels do not vary significantly in position and relative intensity. The nature of these vibronic interactions is presently under investigation.

Finally we note that the intermolecular interactions in the  $h_4$ - and  $d_4$ -homo-dimers are nearly identical.

#### B. Pyrazine- $h_4$ -Pyrazine- $d_4$ Dimer.

The spectra that arise from the isotopic pyrazine hetero-dimer are nearly identical to those of the homo-dimers, independent of which moiety of the dimer is excited. Thus the assignments of the hetero-dimer spectra to particular calculated configurations should follow exactly from the homo-dimer analysis (see fig. 4 and 6). The features at  $-12.2 \text{ cm}^{-1}$  from their respective origins are due to excitation of the planar configuration of the dimer, the features at an average shift of  $-38.2 \pm 0.4 \text{ cm}^{-1}$  are due to excitation of the base molecules in the perpendicular dimer, and the features at an average shift of  $23.5 \pm 0.5 \text{ cm}^{-1}$  are due to excitation of the stem molecules of the perpendicular dimer. The assignments are summarized in Table II and all the pyrazine dimer spectra are compared schematically in fig. 6.

All three pyrazine dimers have, within experimental error, the same shift for the planar configuration feature,  $-11.5 \pm 0.5 \text{ cm}^{-1}$ . Thus deuteration has no effect on the shift or the exciton splitting in the planar hydrogen bonded dimer (fig. 3, I); exciton interaction in this geometry is essentially zero.

As can be seen from Tables I and II, some isotopic shift differences are found for the perpendicular configuration of the pyrazine dimers even though the base-stem splitting remains constant at  $59.5 \pm 1.5 \text{ cm}^{-1}$ . The spectrum of the perpendicular hetero-dimer is red shifted by roughly  $11 \text{ cm}^{-1}$  with respect to that of the homo-dimers. Little or no exciton splitting exists for this configuration: the total hetero-dimer splitting is slightly larger than, but within experimental uncertainty of, the homo-dimer splittings.

#### C. Pyrazine-d<sub>4</sub>-Pyrimidine-h<sub>4</sub> Dimer.

As pointed out in the Results section, the spectrum of the pyrazine-d<sub>4</sub>-pyrimidine hetero-dimer (figs. 5 & 6) is quite complicated. Additional information would be useful in assigning features to the calculated configurations. We thus employ the pyrazine, pyrimidine, and pyrazine-h<sub>4</sub>-pyrimidine dimer spectra to assist with the task.

Examining the stick diagram representation of fig. 6, we can now assign the two features at  $-39.6$  and  $+23.2 \text{ cm}^{-1}$  from the pyrazine-d<sub>4</sub> origin: in accordance with the discussion for the pyrazine dimers these features must be respectively the pyrazine-d<sub>4</sub> moiety in the perpendicular geometry at the base and stem of the pyrazine-d<sub>4</sub>-pyrimidine hetero-dimer. The configurations responsible for these transitions are depicted in fig. 8 and assigned to the spectra in fig. 5 and Table III.

One can properly expect that two such comparable features will arise from the pyrimidine moiety in the perpendicular geometries depicted in fig. 8. In addition, features associated with both pyrazine-d<sub>4</sub> and pyrimidine in the planar (pl) and parallel stacked displaced (pd) configurations are also to be expected.

Many features in the pyrazine-d<sub>4</sub>-pyrimidine spectrum are at shifts (with respect to the pyrimidine monomer  $0^{\circ}$  transition) that are nearly identical to those found in the pyrazine-h<sub>4</sub>-pyrimidine spectrum. These

transitions are of course associated with the pyrimidine moiety in the various dimer configurations. Similarly, features are found in the two spectra that are at similar positions relative to the pyrazine-h<sub>4</sub> or -d<sub>4</sub> monomer origins. The pyrazine-h<sub>4</sub>-pyrimidine spectrum is very congested (even in the 2-color TOFMS because of the identical masses of pyrazine-h<sub>4</sub> and pyrimidine-h<sub>4</sub>) and would be of little pictorial assistance to the reader.

Features that have comparable shifts with respect to the pyrimidine monomer O<sub>0</sub><sup>0</sup> transition in both hetero-dimers are found at shifts of -146.6, -122.1, +219.5 and +261.7 cm<sup>-1</sup> in the pyrazine-d<sub>4</sub> hetero-dimer (fig. 5 and 6 and Table III) and at -155.8, -123.7, +219.6 and +255.7 cm<sup>-1</sup> in the pyrazine-h<sub>4</sub> hetero-dimer (not shown). Once transitions can be associated with a particular molecular component of the dimers the task of assigning the features to a calculated configuration is a relatively straightforward one.

The feature at -146.6 cm<sup>-1</sup> with respect to the pyrimidine monomer origin in the pyrazine-d<sub>4</sub>-pyrimidine hetero-dimer spectrum, the lowest energy feature belonging to the dimer, must be due to the pyrimidine molecule in the parallel displaced geometry. Exciting the pyrazine-d<sub>4</sub> partner in this parallel displaced geometry (fig. 7) yields a feature at -62.7 cm<sup>-1</sup> with respect to the pyrazine-d<sub>4</sub> origin. This latter feature is the most red shifted transition that can be associated with pyrazine in the hetero-dimer and is consequently a reasonable assignment. Comparable features are found at -155.8 and -70.4 cm<sup>-1</sup> (with respect to the two monomer origins) in the pyrazine-h<sub>4</sub>-pyrimidine hetero-dimer spectrum and are also assigned to the parallel stacked displaced configuration.

The features at ca. -122 cm<sup>-1</sup> in both hetero-dimers must be associated with the pyrimidine moiety. Since these are also highly red

shifted peaks, they must involve pyrimidine molecules with their  $\pi$ -systems well "solvated" in the dimers. The only such remaining unassigned calculated geometry is configuration I in fig. 8 with pyrimidine at the base of a perpendicular configuration. These assignments are summarized in fig. 5 and Table III.

Since no perpendicular configurations for the pyrimidine dimer itself are identified<sup>3</sup>, comparisons must be made to the pyrazine dimers for some guidance in assigning the stem features for the perpendicular configurations. The stem molecule of the perpendicular pyrazine dimers is assigned to a blue shifted transition (see Tables I and II). Thus the feature to be associated with pyrimidine at the stem of the perpendicular configurations will likely have a blue shift because its  $\pi$ -electron system is not directly involved in the dimer bonding while its hydrogen atoms are (fig. 8). A blue shifted transition should then occur in both the pyrazine- $h_4$  and pyrazine- $d_4$ -pyrimidine dimers at equal shifts with respect to the pyrimidine monomer  $O_0^0$  transition. The only unique candidate for such an assignment is the feature at  $+219.5 \text{ cm}^{-1}$  in both dimers. While this shift is at first glance rather larger than expected, the assignment is both unique and compelling.

The final calculated configuration that must be assigned to the remaining spectroscopic features is the planar configuration shown in fig. 7. The feature at  $+261.7 \text{ cm}^{-1}$  with respect to the pyrimidine monomer  $O_0^0$  transition in the pyrazine- $d_4$ -pyrimidine dimer and at  $+255.7 \text{ cm}^{-1}$  with respect to the pyrimidine monomer  $O_0^0$  transition in the pyrazine- $h_4$ -pyrimidine dimer is very similar to that found in the pyrimidine dimer at  $+296 \text{ cm}^{-1}$ . Moreover, this transition apparently has associated van der Waals vibrational modes at relative energies of  $38.5$  and  $54.5 \text{ cm}^{-1}$ , just as the pyrimidine dimer feature does.<sup>3</sup> In the pyrimidine dimer the  $296 \text{ cm}^{-1}$  transition is assigned to the planar hydrogen bonded geometry involving the hydrogen atom between the two nitrogens on both pyrimidine molecules (see fig. 7 of ref. 3). Since this

is comparable to the planar structure shown in fig. 7, the ca.  $+260 \text{ cm}^{-1}$  feature of the pyrazine-pyrimidine hetero-dimer is assigned to the pyrimidine moiety of the planar hydrogen bonded hetero-dimer.

The remaining transition to locate for the pyrazine-pyrimidine hetero-dimer is that associated with the pyrazine excitation of the planar hydrogen bonded dimer. Excitation of pyrazine- $\text{h}_4$  or  $-\text{d}_4$  in the planar configuration of the pyrazine homo- and hetero-(isotopic) dimers gives a transition with a shift of  $-11.5 \pm 0.5 \text{ cm}^{-1}$  with respect to the pyrazine monomer  $0_0^0$  transition. Pyrazine in any of the perpendicular hetero-dimers has shifts of  $-38.5 \pm 1.0 \text{ cm}^{-1}$  and  $+23.0 \pm 1.0 \text{ cm}^{-1}$  for the base and stem molecules, respectively. One concludes therefore that pyrazine transitions are not much affected by the other molecular component of the dimer and specifically, that the pyrazine- $\text{d}_4$  planar hydrogen bonded transition of the pyrazine- $\text{d}_4$ -pyrimidine hetero-dimer should be found near the pyrazine- $\text{d}_4$  monomer  $0_0^0$ . The only feature in this region occurs at a shift of  $-0.2 \text{ cm}^{-1}$  and we assign this transition to the pyrazine- $\text{d}_4$  moiety in the pyrazine- $\text{d}_4$ -pyrimidine planar hydrogen bonded dimer. In the pyrazine- $\text{h}_4$ -pyrimidine spectrum the region near the pyrazine- $\text{h}_4$  monomer origin is very congested and a clear assignment is difficult to make for a comparable feature.

The remaining unassigned transitions in the pyrazine- $\text{d}_4$ -pyrimidine spectrum can readily be identified as van der Waals mode vibrations. For example, the weak feature at  $-51.0 \text{ cm}^{-1}$  in fig. 5 is at  $-93.5 \text{ cm}^{-1}$  with respect to the pyrimidine monomer origin. A comparable feature is found in the pyrazine- $\text{h}_4$ -pyrimidine dimer at  $-94.2 \text{ cm}^{-1}$ . The transition can be assigned as a van der Waals mode built on the pyrimidine perpendicular base (Ib in fig. 5 and Table III) origin at ca.  $-122 \text{ cm}^{-1}$ . The six features following the

pyrimidine planar transition at ca.  $300\text{ cm}^{-1}$  in fig. 5 ( $261.7\text{ cm}^{-1}$  from the pyrimidine monomer  $0_0^0$  transitions) can also be assigned as van der Waals modes of the planar hydrogen bonded pyrazine-pyrimidine hetero-dimer.

In general, substituting pyrazine- $h_4$  for pyrazine- $d_4$  in the pyrazine-pyrimidine dimer affects some spectral features more than others. For example, in the parallel displaced configuration the two features are shifted  $+8.5 \pm 0.5\text{ cm}^{-1}$  in the  $d_4$  dimer ( $-146.6$  and  $-62.5\text{ cm}^{-1}$ ) with respect to the  $h_4$  dimer ( $-155.8$  and  $-70.4\text{ cm}^{-1}$ ) even though the overall dimer splitting is nearly constant at  $84.8 \pm 0.6\text{ cm}^{-1}$ . A comparable effect ( $+6\text{ cm}^{-1}$  shift) exists for the  $h_4$  and  $d_4$  dimers of the planar configuration ( $255.7\text{ cm}^{-1}$  for  $h_4$  and  $261.7\text{ cm}^{-1}$  for  $d_4$ ). Transitions of the perpendicular configurations, however, have nearly identical positions ( $-122.9 \pm 0.8\text{ cm}^{-1}$ ,  $+219.5\text{ cm}^{-1}$ ,  $-39.5\text{ cm}^{-1}$  and  $-23.7 \pm 0.3\text{ cm}^{-1}$ ).

#### V. Conclusions.

The pyrazine homo- and hetero- isotopic dimers form a set of dimers whose spectra and structure now seem to be quite well understood. Two configurations are calculated and assigned from the spectra: a planar hydrogen bonded geometry and a perpendicular geometry. A third configuration, parallel stacked, rotated  $90^\circ$ , is also calculated for pyrazine dimers but not observed spectroscopically. The interaction strengths (that is, splittings for the perpendicular dimer and energy of the single feature for the planar dimer with respect to the appropriate monomer origin) do not seem to depend on the isotopic composition of the dimer. This strongly implies that the exciton or exchange interactions for this system are vanishingly small (less than  $1\text{ cm}^{-1}$ ). The general red and blue shifts of the dimer features with respect to the monomer origins are consistent with the  $\pi$ -system coordination and electron donor-acceptor (hydrogen bonding) behavior found for solute/solvent complexes.

The pyrazine-pyrimidine hetero-dimer falls into this general pattern as well, and its spectra can be assigned with some certainty. Parallel stacked displaced, perpendicular, and planar hydrogen bonded configurations can be calculated and identified experimentally for this dimer. In all five distinct configurations can be assigned for the pyrazine-pyrimidine dimer.

The pyrimidine dimer itself has been previously found to have six configurations: a parallel stacked head-to-tail displaced dimer, a parallel stacked rotated  $90^\circ$  dimer, and four planar hydrogen bonded dimers. Apparently heterocyclic dimer geometry is very rich and a number of different configurations are stable for each system.

## REFERENCES

1. a. K.S. Law, M. Schauer, and E.R. Bernstein, *J. Chem. Phys.* 81, 4871 (1984).  
b. C.A. Hayman, D.V. Brumbaugh, and D.H. Levy, *J. Chem. Phys.* 79, 1581 (1983).  
c. D.E. Poeltl and J.K. McVey, *J. Chem. Phys.* 78, 4349 (1983).  
d. Y. Tomioka, H. Abe, N. Mikami, and M. Ito, *J. Phys. Chem.* 88, 5186 (1984).  
e. K.O. Boernsen, H.L. Selzle, and E.W. Schlag, *Z. Naturforsch.*, 39A, 1255 (1984).
2. M. Schauer and E.R. Bernstein, *J. Chem. Phys.* 82, 3722 (1985).
3. J. Wanna, J. Menapace, and E.R. Bernstein, *J. Chem. Phys.* submitted.
4. J. Wanna and E.R. Bernstein, *J. Chem. Phys.* 84, 927 (1986).
5. a. M. Schauer and E.R. Bernstein, *J. Chem. Phys.* 82, 726 (1985).  
b. M. Schauer, K. Law, and E.R. Bernstein, *J. Chem. Phys.* 81, 49 (1984).
6. a. F.A. Monomany, L.M. Carruthers, R.F. McGuire, and H.A. Scheraga, *J. Phys. Chem.* 78, 1595 (1974).  
b. G. Nemethy, M.S. Pottle, and H.A. Scheraga, *J. Phys. Chem.* 87, 1883 (1983).

Table I  
Pyrazine-d<sub>4</sub> Dimer

Energy (vac. cm <sup>-1</sup> )	Energy Relative to Corresponding Pyrazine-d <sub>4</sub> Feature (cm <sup>-1</sup> )	Energy Relative to Corresponding Pyrazine-d <sub>4</sub> Dimer Feature (cm <sup>-1</sup> )	Assignment <sup>a, b</sup>
31003.5	-26.9	0	II base 0 <sub>0</sub> <sup>0</sup>
31018.9	-11.5	0	I 0 <sub>0</sub> <sup>0</sup>
31024.0	- 6.4	20.5	
31041.9	11.5	23.0	
31055.9	25.5	37.0	
31061.4	31.0	0	II stem 0 <sub>0</sub> <sup>0</sup>
31076.3	45.9	14.9	
31081.4	51.0	20.0	
31094.5	64.1	33.1	
31296.6	-26.4	0	II base 10a <sub>0</sub> <sup>1</sup>
31310.5	-12.5	0	I 10a <sub>0</sub> <sup>1</sup>
31356.6	33.6	0	II stem 10a <sub>0</sub> <sup>1</sup>
31566.4	-28.9	0	II base 6a <sub>0</sub> <sup>1</sup>
31572.2	-23.1	5.8	
31582.9	-12.4	0	I 6a <sub>0</sub> <sup>1</sup>
31632.5	37.2	0	II stem 6a <sub>0</sub> <sup>1</sup>
31646.0	50.7	13.5	

<sup>a</sup> See figure 3.

<sup>b</sup> Peaks at shifts of -11.5, 11.5, 25.5, and 64.1 cm<sup>-1</sup> vanish at the lower ionization energy (42300 cm<sup>-1</sup>).

Table II  
 Pyrazine-d<sub>4</sub>-Pyrazine-h<sub>4</sub>

Energy (vac. cm <sup>-1</sup> )	Energy Relative to Corresponding 0 <sub>0</sub> <sup>0</sup> of the Excited Molecule of the Dimer (cm <sup>-1</sup> )	Energy Relative to Corresponding Dimer Feature (cm <sup>-1</sup> )	Assignment <sup>a</sup>
30991.8	-38.4	0	II base 0 <sub>0</sub> <sup>0</sup>
31018.0	-12.2	0	I 0 <sub>0</sub> <sup>0</sup>
31040.4	10.0	22.4	
31054.2	24.0	0	II stem 0 <sub>0</sub> <sup>0</sup>
31061.8	31.4	7.6	
31081.5	51.1		
31108.0	77.6		
31230.7	200.3		
Pyrazine-d <sub>4</sub> -Pyrazine-h <sub>4</sub> <sup>*</sup>			
30838.1	-37.9	0	II base 0 <sub>0</sub> <sup>0</sup>
30863.8	-12.2	0	I 0 <sub>0</sub> <sup>0</sup>
30899.0	23.0	0	II stem 0 <sub>0</sub> <sup>0</sup>
30908.3	32.3	9.3	
30918.9	42.9		
30925.6	49.6		

<sup>a</sup> See figure 3.

Table III  
 Pyrazine-d<sub>4</sub>-Pyrimidine Dimer Origins only.

Energy (vac. cm <sup>-1</sup> )	Energy Relative to Pyrazine-d <sub>4</sub> O <sub>0</sub> (cm <sup>-1</sup> )	Energy Relative to Pyrimidine O <sub>0</sub> (cm <sup>-1</sup> )	Assignment <sup>a</sup>
30926.1		-146.6	pdy pyrimidine parallel displaced
30950.6		-122.1	Ib pyrimidine base
30967.7	-62.7		pdz pyrazine parallel displaced
30979.2		- 93.5	
30990.8	-39.6		II, IIIb pyrazine base
31030.2	- 0.2		pz pyrazine planar
31053.6	23.2		Is pyrazine stem
31061.8	31.4		
31292.2		219.5	II, IIIs pyrimidine stem
31334.4		261.7	py pyrimidine planar

<sup>a</sup> See figures 5, 7, and 8.

## FIGURES

- Figure 1 Two-color TOFMS of pyrazine-d<sub>4</sub> dimer in the region of the pyrazine-d<sub>4</sub> origin. Spectra taken with two different ionization energies are presented. The pyrazine-d<sub>4</sub> monomer origin (31030.4 cm<sup>-1</sup>) lies at 0 cm<sup>-1</sup> on the scale of the figure. See Table I for absolute energies.
- Figure 2 Two-color TOFMS of the pyrazine-d<sub>4</sub> dimer in the O<sub>0</sub><sup>0</sup>, 10a<sub>0</sub><sup>1</sup>, and 6a<sub>0</sub><sup>1</sup> regions. See Table I for absolute energies. The high ionization energy of fig. 1 is employed.
- Figure 3 Minimum energy configurations and binding energies for the spectroscopically observed pyrazine dimers as obtained with the LJ-HB potential calculation.
- Figure 4 Top: 2-color TOFMS of pyrazine-h<sub>4</sub>-pyrazine-d<sub>4</sub> dimer exciting pyrazine-d<sub>4</sub> moiety. Bottom: 2-color TOFMS of pyrazine-h<sub>4</sub>-pyrazine-d<sub>4</sub> dimers exciting pyrazine-h<sub>4</sub> moiety. Scale relative to either monomer origin located at 0 cm<sup>-1</sup> (d<sub>4</sub> O<sub>0</sub><sup>0</sup> at 31030.4 cm<sup>-1</sup> and h<sub>4</sub> O<sub>0</sub><sup>0</sup> at 30876.0 cm<sup>-1</sup>). Ionization energy employed to obtain these spectra is 43598 cm<sup>-1</sup>.
- Figure 5 2-color TOFMS of pyrazine-d<sub>4</sub>-pyrimidine dimer shown in two segments. Scale relative to the pyrazine-d<sub>4</sub> monomer origin (31030.4 cm<sup>-1</sup>) located at 0 cm<sup>-1</sup> in the figure. The assignment codes refer to dimer configuration and a particular member of the dimer: pdy stands for parallel displaced pyrimidine, pdz

for parallel displaced pyrazine, py for planar pyrimidine, pz for planar pyrazine, Ib and Is for configuration I base and stem respectively, II, III b and II, III s for either configuration II or III base and stem respectively. These calculated geometries are displayed in figures 7 and 8.

Figure 6 Stick diagram showing features associated with the different dimers. The top diagram represents pyrazine-h<sub>4</sub> dimer and pyrazine-d<sub>4</sub> dimer. Dashed lines identify the three origins of the monomers involved: pyrazine-h<sub>4</sub> at 30876 cm<sup>-1</sup>, pyrazine-d<sub>4</sub> at 31030.4 cm<sup>-1</sup>, and pyrimidine at 31072.7 cm<sup>-1</sup>. The middle diagram represents the dimer pyrazine-h<sub>4</sub>-pyrazine-d<sub>4</sub>: first part exciting pyrazine-h<sub>4</sub> and second part exciting pyrazine-d<sub>4</sub>. The bottom diagram represents the pyrazine-d<sub>4</sub>-pyrimidine dimer.

Figure 7 Two minimum energy configurations and binding energies for pyrazine-pyrimidine dimer as obtained with a LJ-HB potential calculation.

Figure 8 Three perpendicular minimum energy configurations and binding energies for pyrazine-pyrimidine dimer as obtained with a LJ-HB potential calculation.

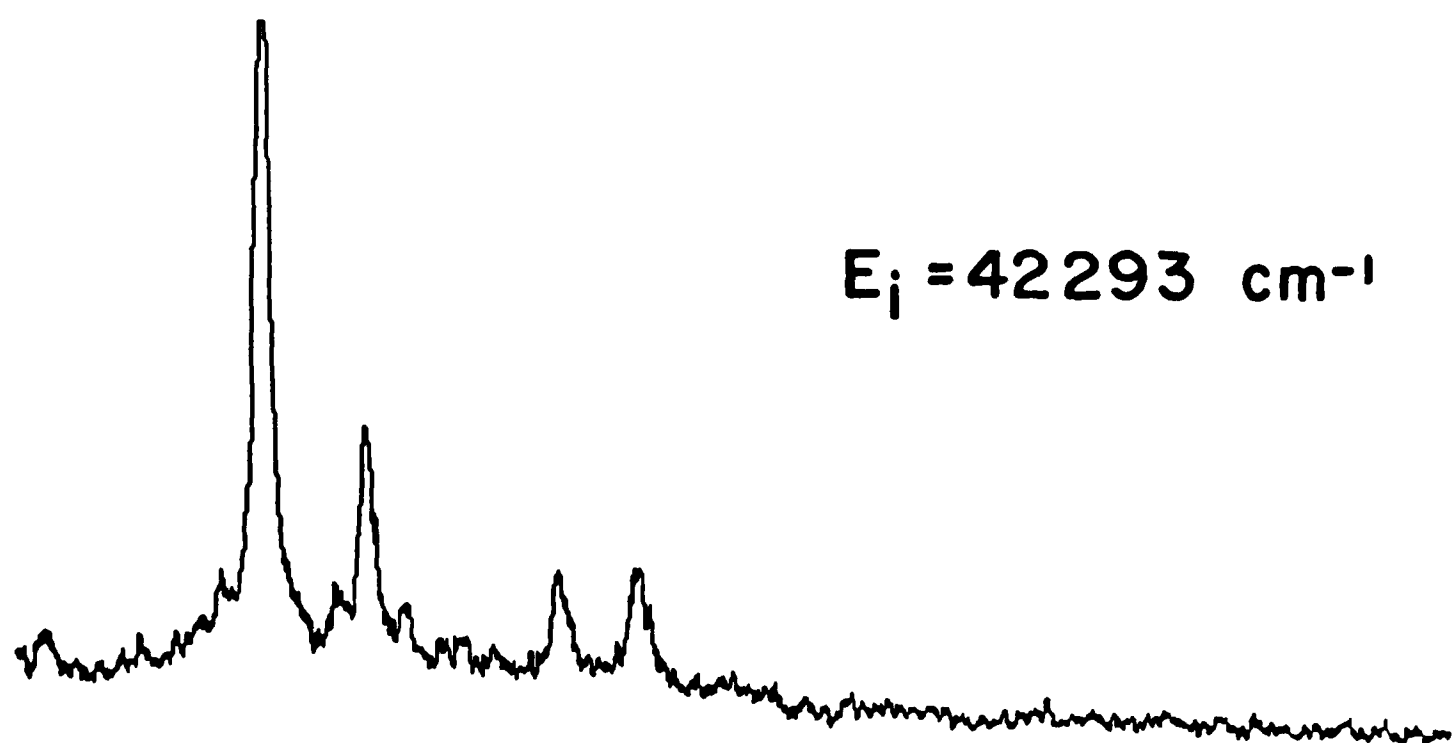
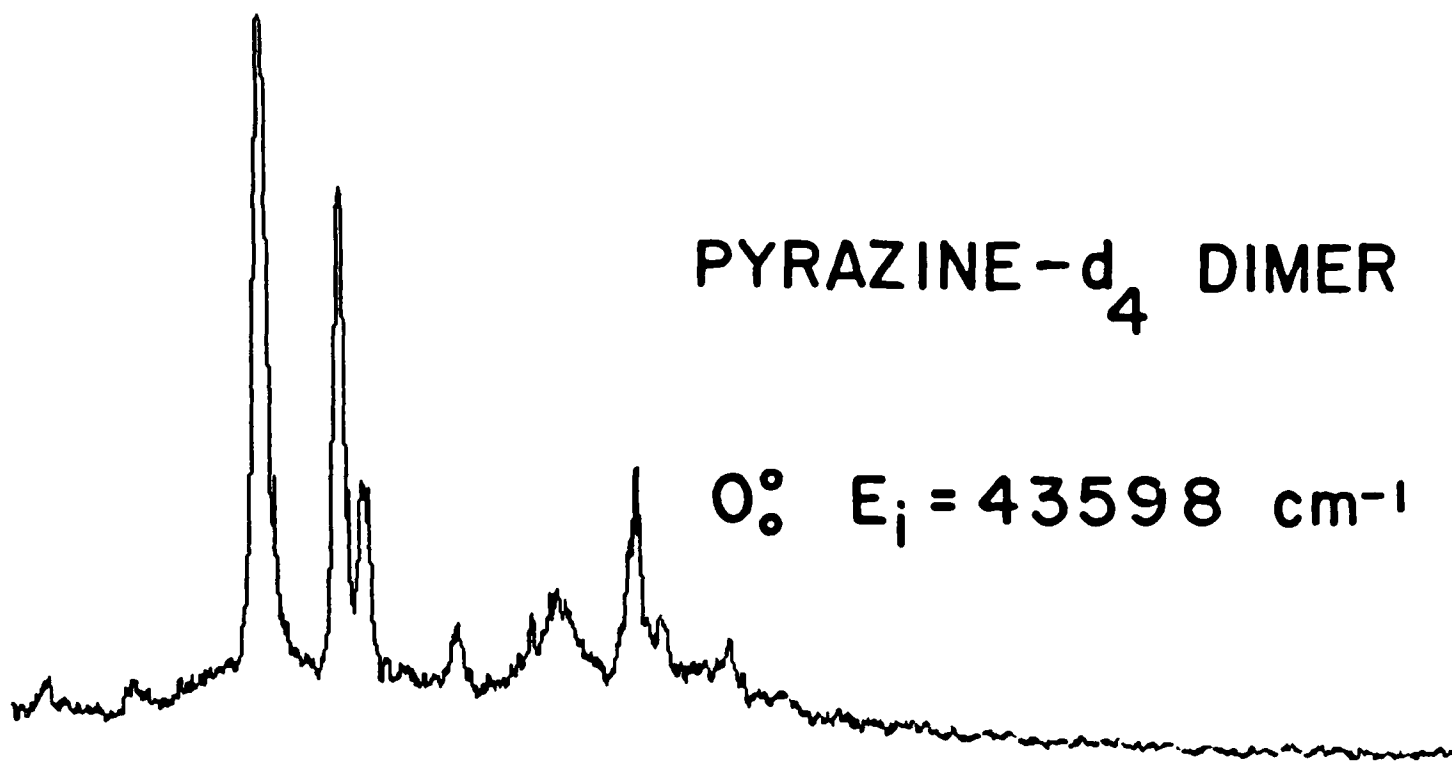
PYRAZINE-d<sub>4</sub> DIMER

0° E<sub>i</sub> = 43598 cm<sup>-1</sup>

E<sub>i</sub> = 42293 cm<sup>-1</sup>

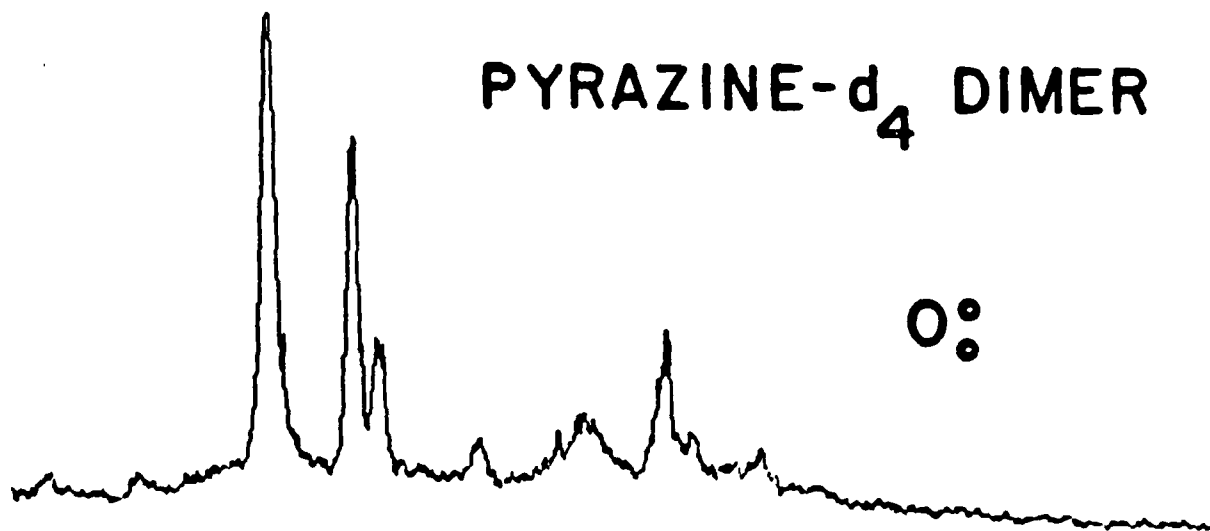
-50 0 +50

RELATIVE ENERGY (cm<sup>-1</sup>)

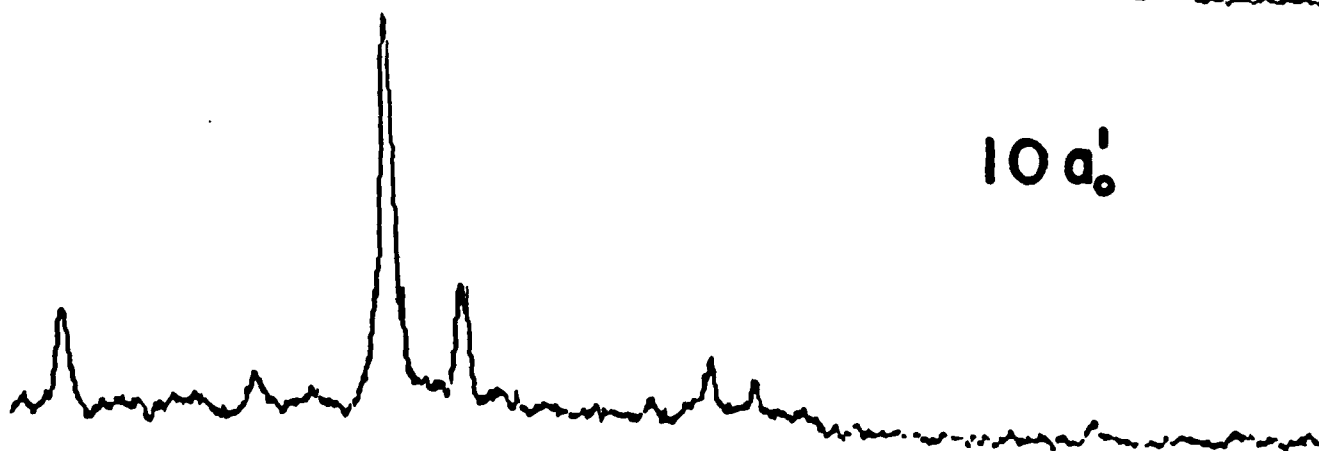


PYRAZINE-d<sub>4</sub> DIMER

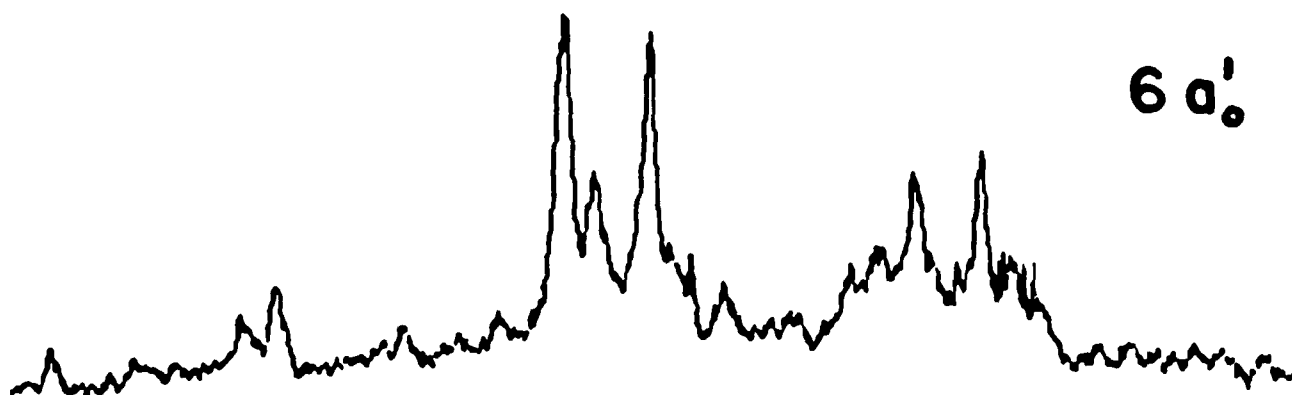
0°



10 a'



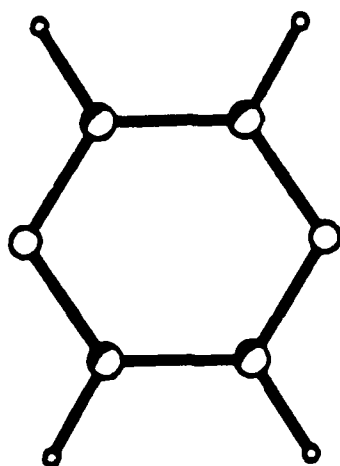
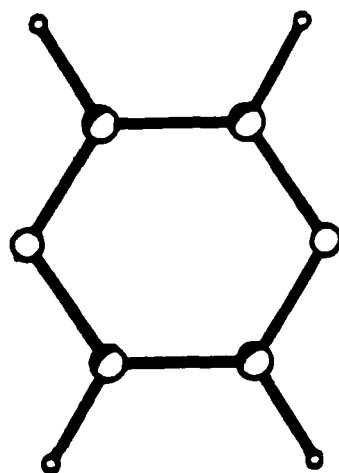
6 a'



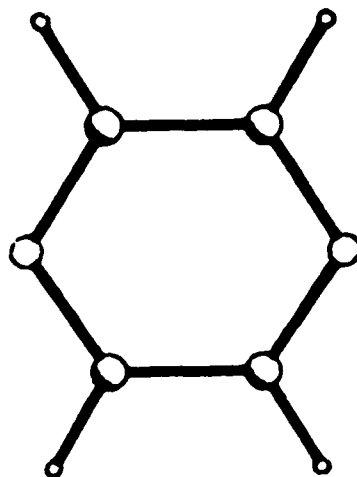
0 +40 +80

RELATIVE ENERGY (cm<sup>-1</sup>)

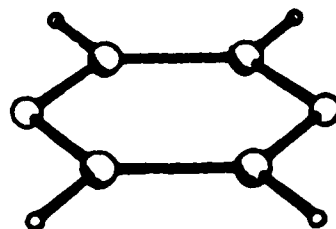
# PYRAZINE DIMER



I - 716  $\text{cm}^{-1}$



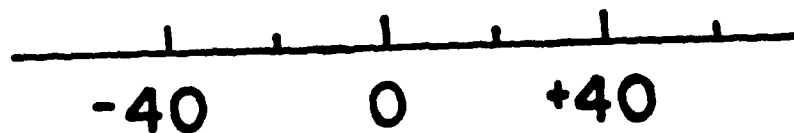
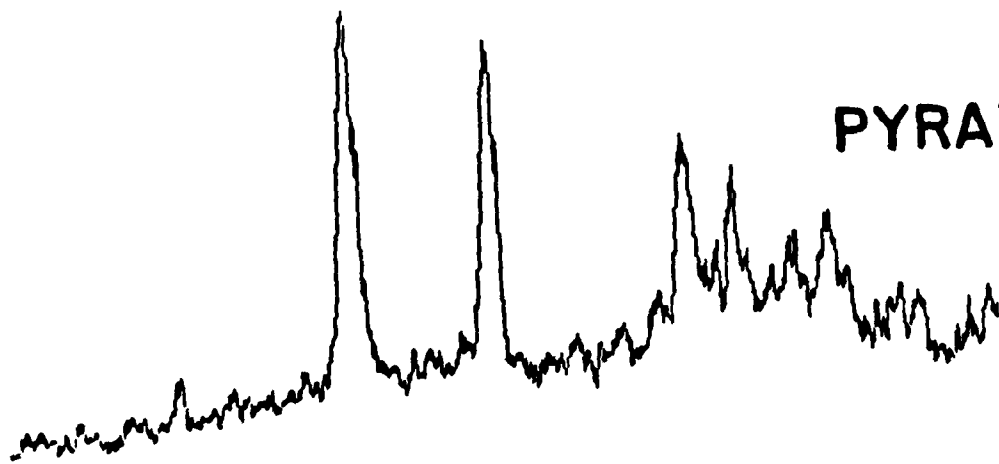
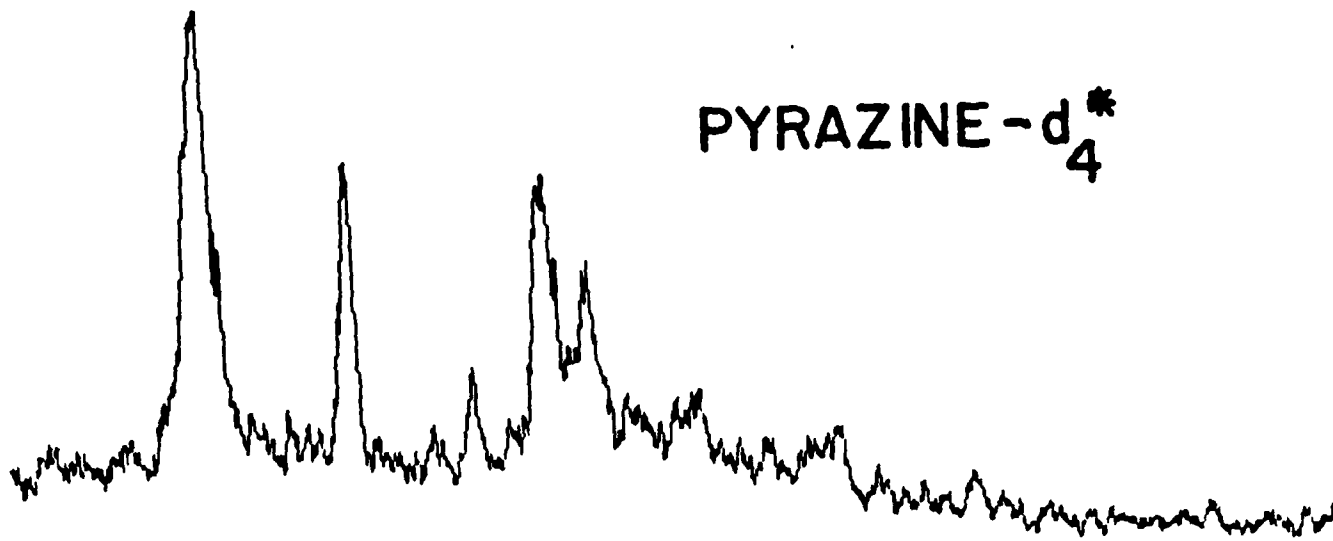
II - 854  $\text{cm}^{-1}$



PYRAZINE- $h_4, d_4$  DIMER

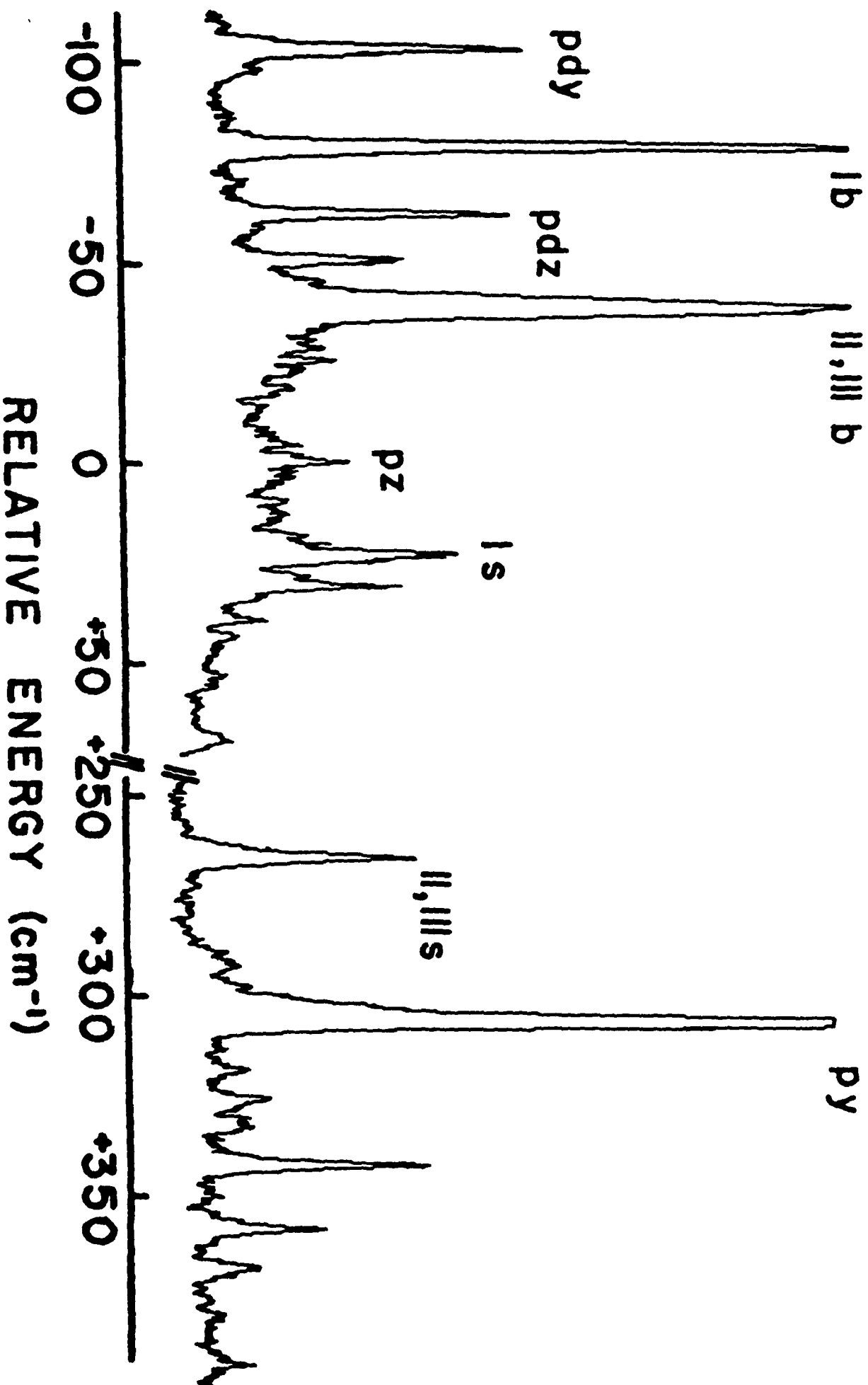
PYRAZINE- $d_4^*$

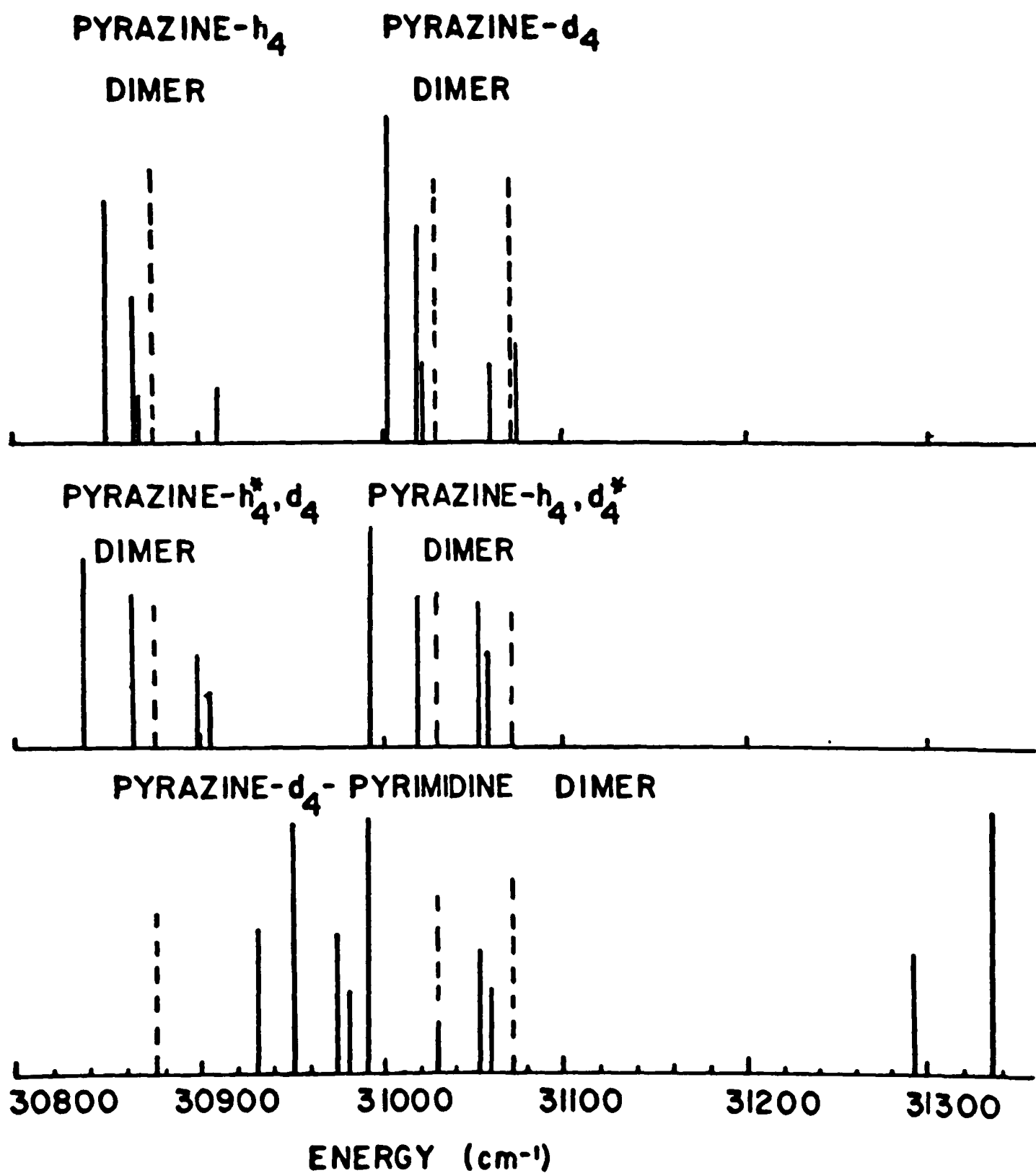
PYRAZINE- $h_4^*$



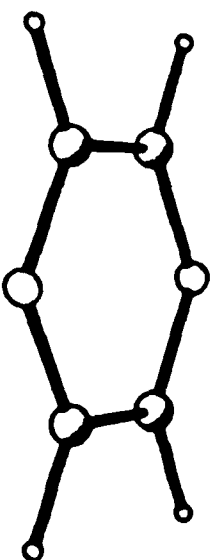
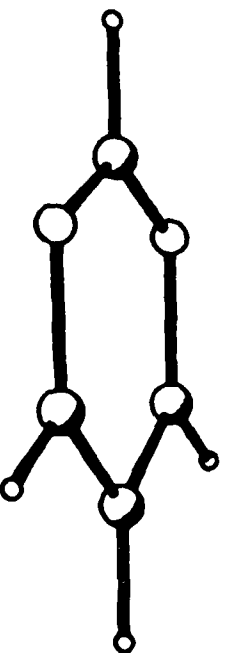
RELATIVE ENERGY (cm<sup>-1</sup>)

# PYRAZINE- $d_4$ -PYRIMIDINE DIMER

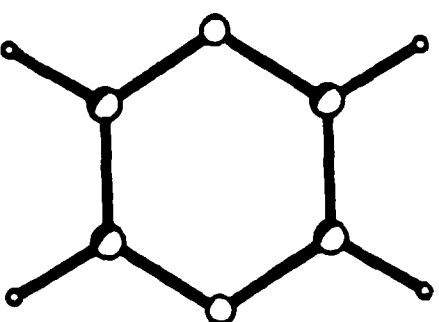




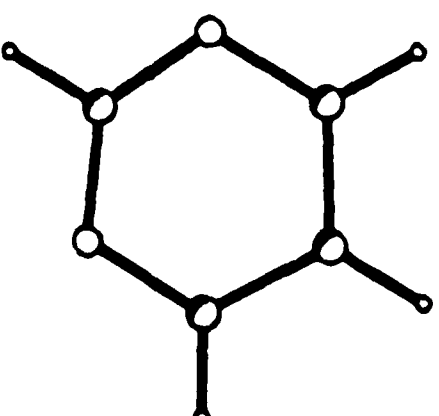
# PYRAZINE-PYRIMIDINE DIMER



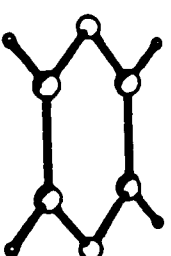
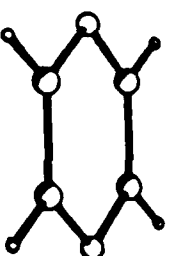
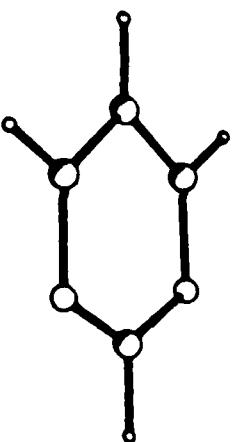
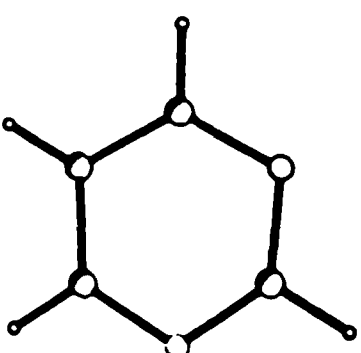
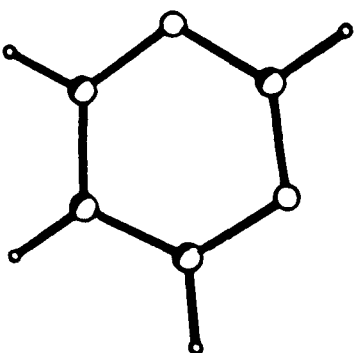
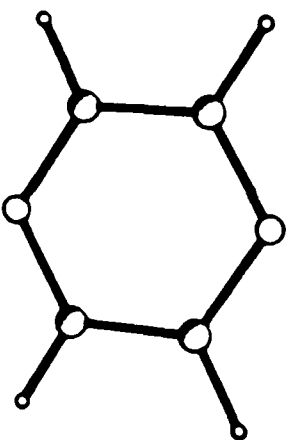
-1437  $\text{cm}^{-1}$



-614  $\text{cm}^{-1}$



# PYRAZINE-PYRIMIDINE DIMER



I - 841  $\text{cm}^{-1}$

II - 723  $\text{cm}^{-1}$

III - 721  $\text{cm}^{-1}$

TECHNICAL REPORT DISTRIBUTION LIST, GEN

	<u>No. Copies</u>		<u>No. Copies</u>
Office of Naval Research Attn: Code 413 800 N. Quincy Street Arlington, Virginia 22217	2	Dr. David Young Code 334 NORDA NSTL, Mississippi 39529	1
Dr. Bernard Douda Naval Weapons Support Center Code 5042 Crane, Indiana 47522	1	Naval Weapons Center Attn: Dr. A. B. Amster Chemistry Division China Lake, California 93555	1
Commander, Naval Air Systems Command Attn: Code 310C (H. Rosenwasser) Washington, D.C. 20360	1	Scientific Advisor Commandant of the Marine Corps Code RD-1 Washington, D.C. 20380	1
Naval Civil Engineering Laboratory Attn: Dr. R. W. Drisko Port Hueneme, California 93401	1	U.S. Army Research Office Attn: CRD-AA-IP P.O. Box 12211 Research Triangle Park, NC 27709	1
Defense Technical Information Center Building 5, Cameron Station Alexandria, Virginia 22314	12	Mr. John Boyle Materials Branch Naval Ship Engineering Center Philadelphia, Pennsylvania 19112	1
DTNSRDC Attn: Dr. G. Bosmajian Applied Chemistry Division Annapolis, Maryland 21401	1	Naval Ocean Systems Center Attn: Dr. S. Yamamoto Marine Sciences Division San Diego, California 91232	1
Dr. William Tolles Superintendent Chemistry Division, Code 6100 Naval Research Laboratory Washington, D.C. 20375	1		

ABSTRACTS DISTRIBUTION LIST, 051A

Dr. M. A. El-Sayed  
Department of Chemistry  
University of California  
Los Angeles, California 90024

Dr. E. R. Bernstein  
Department of Chemistry  
Colorado State University  
Fort Collins, Colorado 80521

Dr. J. R. MacDonald  
Chemistry Division  
Naval Research Laboratory  
Code 6110  
Washington, D.C. 20375

Dr. G. B. Schuster  
Chemistry Department  
University of Illinois  
Urbana, Illinois 61801

Dr. W. M. Jackson  
Department of Chemistry  
Howard University  
Washington, D.C. 20059

Dr. M. S. Wrighton  
Department of Chemistry  
Massachusetts Institute of Technology  
Cambridge, Massachusetts 02139

Dr. A. Paul Schaap  
Department of Chemistry  
Wayne State University  
Detroit, Michigan 49207

Dr. Gary Bjorklund  
IBM  
5600 Cottle Road  
San Jose, California 95143

Dr. G. A. Crosby  
Chemistry Department  
Washington State University  
Pullman, Washington 99164

Dr. W. E. Moerner  
I.B.M. Corporation  
5600 Cottle Road  
San Jose, California 95193

Dr. Theodore Pavlopoulos  
NOSC  
Code 5132  
San Diego, California 91232

Dr. D. M. Burland  
IBM  
San Jose Research Center  
5600 Cottle Road  
San Jose, California 95143

Dr. John Cooper  
Code 6170  
Naval Research Laboratory  
Washington, D.C. 20375

Dr. George E. Walrafen  
Department of Chemistry  
Howard University  
Washington, D.C. 20059

Dr. Joe Brandelik  
AFWAL/AADO-1  
Wright Patterson AFB  
Fairborn, Ohio 45433

Dr. Carmen Ortiz  
Consejo Superior de  
Investigaciones Cientificas  
Serrano 117  
Madrid 6, SPAIN

Dr. John J. Wright  
Physics Department  
University of New Hampshire  
Durham, New Hampshire 03824

Dr. Kent R. Wilson  
Chemistry Department  
University of California  
La Jolla, California 92093

END

10 - 86

DTIC